Simulation of 2D Axisymmetric GaAs P-N Junction Infrared LED and Study on Spatial Distribution of Emissivity

DOI: 10.23977/jeeem.2025.080118

ISSN 2560-6697 Vol. 8 Num. 1

Shaolong Liu¹, Wen Li^{1,*}, Xinyu Miao², Tiansheng Sun¹

¹School of Electrical Engineering, Yingkou Institute of Technology, Yingkou, 115000, China ²Yingkou Abe Wiring Co., Ltd., Yingkou, 115000, China *Corresponding author: 1609151361@qq.com

Keywords: GaAs P-N Junction; Infrared LED; 2D Axisymmetric Modeling; Spatial Distribution of Emissivity; Auger Recombination

Abstract: To investigate the electrical characteristics and light emission laws of gallium arsenide (GaAs) P-N junction infrared light-emitting diodes (LEDs), particularly the influence of the spatial distribution of emissivity on device efficiency, this study adopts a 2D axisymmetric modeling approach for simulation. The device is based on a 60µmdiameter circular GaAs chip, and the 2D model is simplified to a rectangular structure with a thickness of 10 µm and a width of 30 µm. The top 2.5 µm layer is p-type doped (concentration: 1×10^{18} cm⁻³), while the bottom 7.5 µm layer is n-type doped (concentration: 1×10¹⁸ cm⁻³). The Auger recombination non-radiative mechanism is introduced to simulate the efficiency degradation process. The simulation first uses a "semiconductor initialization study" to automatically refine the mesh around the P-N junction, followed by a steady-state study with a bias voltage scan from 0 V to 1.5 V to analyze the current-voltage (I-V) characteristics, spatial distribution of emissivity, and variation law of internal quantum efficiency (IQE). The results show that: the turn-on voltage of the device is approximately 1.2 V; under low current (<5 mA, corresponding to a bias voltage of 1.2-1.3 V), the emission is distributed uniformly across the entire p-type layer, and the IQE remains at a high level; under high bias voltage (e.g., 1.5 V), the emission concentrates beneath the central p-type contact, the total emissivity increases sublinearly with current, and the IQE drops sharply to 0.075 as current increases (attributed to the Auger recombination rate being proportional to the cube of carrier density, which enhances the proportion of non-radiative recombination). The 2D axisymmetric modeling significantly reduces the computational load while accurately capturing the key performance laws of the device. The research results provide a basis for the design optimization of household infrared devices (such as remote controls and night-vision cameras): a bias voltage of 1.2-1.3 V can be selected for low-power scenarios, and transparent p-type contacts or annular contact designs are required to improve light extraction efficiency for high-brightness scenarios.

1. Introduction

Infrared light-emitting diodes (LEDs), as core devices in the field of photoelectric conversion (as shown in Figure 1), have been widely used in consumer electronics, security monitoring, and other fields due to their low power consumption, long lifespan, and narrow-band emission characteristics[1]. Among them, household devices such as TV remote controls and smart device sensors impose strict requirements on device cost and manufacturing complexity. Although complex heterojunction or quantum well structures can improve luminous efficiency, they are costly due to cumbersome processes[2]. In contrast, the simple gallium arsenide (GaAs) P-N junction structure has become the mainstream choice for such household infrared devices, thanks to its simple preparation process and low raw material cost.

However, GaAs P-N junction infrared LEDs face key challenges in practical applications: as the operating current increases, non-radiative recombination of carriers intensifies, leading to a significant decline in luminous efficiency[3]; meanwhile, the spatial distribution of device emissivity is closely related to the design of contact structures, and opaque metal contacts may block the core light-emitting area, further reducing the actual light extraction efficiency[4]. These issues directly affect the battery life and functional stability of household devices, highlighting the urgent need for accurate modeling and simulation analysis to reveal the intrinsic laws of their electrical and optical characteristics[5].



Figure 1 Schematic diagram of the LED structure

In the research on GaAs P-N junction infrared LEDs, simulation technology has become a core means to optimize device performance. Traditional full 3D modeling can fully restore the device structure but consumes substantial computational resources[6]. Particularly in bias voltage scanning and mesh refinement analysis, the long computation cycle limits the efficiency of multi-scheme comparison[7]; while simplified 1D modeling reduces computational cost, it cannot accurately capture the spatial distribution characteristics of emissivity, making it difficult to support the optimization design of contact structures[8].

Current studies mostly focus on the simulation verification of single electrical characteristics (e.g., I-V curves), with insufficient analysis of the coupling relationship among "current density-internal quantum efficiency-emissivity distribution"[9]. Additionally, the quantitative impact of non-radiative recombination mechanisms (such as Auger recombination) is not clearly defined, leading to deviations between simulation results and actual device performance[10]. Furthermore, there is limited research on device parameter adaptation for different application scenarios of household devices (e.g., low-power requirements for remote controls and high-brightness requirements for night-vision cameras), making it difficult to provide targeted design guidance. This underscores the urgency of conducting accurate and efficient simulation research.

Against this background, this study adopts a 2D axisymmetric modeling approach to simulate the electrical and optical characteristics of GaAs P-N junction infrared LEDs. This modeling method balances computational efficiency and analysis accuracy: through cylindrical symmetry

simplification, it significantly reduces the computational load while fully retaining key information on the spatial distribution of emissivity; meanwhile, the Auger recombination mechanism is introduced to quantify the impact of non-radiative recombination on efficiency, and adaptive mesh refinement in the P-N junction area is achieved through a semiconductor initialization study to improve the accuracy of simulation results.

By scanning the bias voltage from 0 V to 1.5 V, this study analyzes the turn-on characteristics of the device, the spatial distribution law of emissivity, and the variation trend of internal quantum efficiency. Finally, optimization schemes are proposed for different household scenarios: determining the optimal operating bias voltage range for low-power scenarios and proposing improvement directions for contact structures for high-brightness scenarios. This research not only provides theoretical support for the performance optimization of GaAs P-N junction infrared LEDs but also enables pre-verification of design schemes through simulation, reducing the trial-and-error cost of physical manufacturing. It holds significant practical value for promoting the development of high-efficiency and low-cost household infrared optoelectronic devices.

2. Geometric Construction and Boundary Conditions of the Model

2.1 Geometric Model Construction

To accurately simulate the characteristics of the GaAs P-N junction infrared LED, a 2D axisymmetric model (with the r=0 axis as the axis of symmetry) is adopted based on the circular structure (60µm in diameter) and cylindrical symmetric light-emitting characteristics of the actual device. This ensures simulation accuracy while significantly reducing computational load. The geometric construction focuses on three aspects: overall domain definition, doped region division, and contact structure design.

The overall domain is simplified to a rectangle with a domain width (wdom) of $25\mu m$ and a domain height (hdom) of $10\mu m$. The default physics-induced mesh is set to the "Finer" level (as shown in Figure 2), and the mesh in the P-N junction area is automatically refined through a "semiconductor initialization study" (as shown in Figure 3). Since this area is the core of carrier recombination and light emission with a large doping concentration gradient, higher resolution is required to capture the carrier dynamics process. The mesh density after refinement is 3-5 times higher than that in other regions.

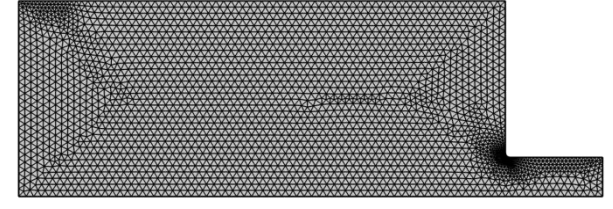


Figure 2 Default physics-induced mesh with the size node set to "Finer"

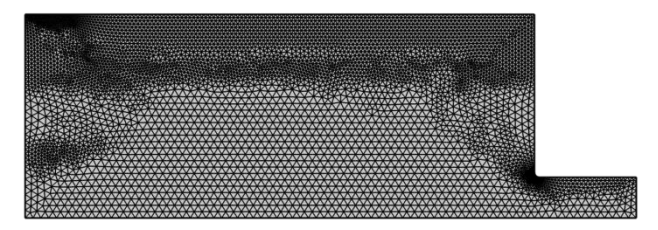


Figure 3 Refined mesh output from the "Semiconductor Initialization" study step in the first study

The doped region adopts a layered design of "top p-type + bottom n-type": the top p-type region

has a thickness (hp) of $2.5\mu m$ and is acceptor-doped (concentration NA0=1×10¹⁸ cm⁻³); the bottom n-type region has a thickness of $7.5\mu m$ and is donor-doped (concentration ND0= 1×10¹⁸ cm⁻³). Both regions use the "decay length" mode (decay length ld=2 μm) to form a smoothly transitioned active light-emitting area (Figure 4).

The contact structure is designed as "central p-type contact + edge n-type contact": the p-type contact is a metal disk at the center of the top surface (appearing as a rectangular segment in the 2D model) with a width (wcon-p) of $2.5\mu m$; the n-type contact is an edge metal ring formed by etching a rectangular groove (width wcon-n= $5\mu m$, height hcon-n= $2\mu m$) in the n-type layer on the right side of the domain. Meanwhile, the edge of the p-type contact is rounded (radius rfill= $0.25\mu m$) to avoid electric field concentration. The overall configuration of the device (2D cross-section and 3D structure) is shown in Figure 4, providing a clear geometric basis for subsequent simulations.

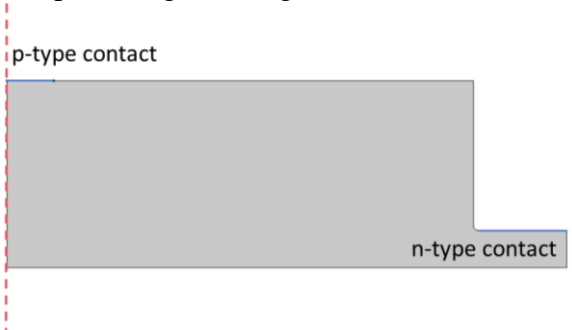


Figure 4 Geometric shape of the device

2.2 Material Parameter Configuration

Material parameters of gallium arsenide (GaAs) are configured to provide a physical basis for simulating the electrical transmission and light-emitting characteristics of the device. All parameters are determined based on semiconductor material handbook data and simulation requirements, focusing on carrier behavior and recombination mechanisms. The specific parameter settings are shown in Table 1.

Parameter Category	Parameter Name	Variable	Value	Unit	Description
Basic Property	Carrier Statistics Model	-	Fermi- Dirac	-	Adapted to carrier distribution in heavily doped semiconductors
Auger Recombination	Electron Auger Recombination Coefficient	C_n	1×10 ⁻³¹	cm ⁶ /s	Simulates electron-dominated non- radiative recombination
	Hole Auger Recombination Coefficient	C_p	1×10 ⁻³¹	cm ⁶ /s	Simulates hole-dominated non-radiative recombination
Doping Parameter	p-type Acceptor Concentration	$N_{ m A0}$	1×10 ¹⁸	cm ⁻³	Doping concentration of the top p-type region
	n-type Donor Concentration	$N_{ m D0}$	1×10 ¹⁸	cm ⁻³	Doping concentration of the bottom n- type region
	Doping Decay Length	l_d	2	μm	Controls the width of the p-n junction transition region

Table 1 Key parameter configuration of GaAs material

For GaAs, the core material of the device, the "Fermi-Dirac" distribution is selected as the carrier statistics model. Since the doping concentrations of both p-type and n-type regions reach 1×10^{18} cm⁻³ (heavily doped), the Fermi-Dirac distribution can more accurately describe the occupancy

characteristics of carriers in energy levels, avoiding calculation deviations under non-degenerate approximation.

In the non-radiative recombination mechanism, the Auger recombination feature is mainly introduced, with both the electron Auger recombination coefficient (Cn) and hole Auger recombination coefficient (Cp) set to 1×10^{-31} cm⁶/s. This value is consistent with the typical Auger coefficient range of GaAs materials. Since the Auger recombination rate is proportional to the cube of the carrier density, it can accurately capture the efficiency degradation phenomenon caused by intensified non-radiative recombination under high current injection, which is consistent with the performance degradation law of actual devices.

The configuration of doping parameters matches the layered design in the geometric structure: the p-type acceptor concentration (NA0) and n-type donor concentration (ND0) are both set to 1×10^{18} cm⁻³, and a doping decay length of $2\mu m$ is used to form a smoothly transitioned interface between the p-type and n-type regions. This avoids carrier transport barriers caused by abrupt doping, thereby constructing an active light-emitting area with a width of approximately 4-5 μm .

The coordinated setting of these parameters ensures that the electrical and optical characteristics of the material in the simulation conform to the physical nature of actual GaAs devices, providing key support for the accuracy of subsequent simulation results such as I-V characteristics and emissivity distribution.

3. Analysis of Simulation Results

3.1 Analysis of Current-Voltage (I-V) Characteristics

The electrical performance of the GaAs P-N junction infrared LED is directly determined by its internal doping structure, and the current-voltage (I-V) curve is an intuitive reflection of its electrical characteristics. This section clarifies the intrinsic relationship between the two and the core electrical laws of the device through a combined analysis of the device doping distribution diagram (Figure 5) and I-V characteristic diagram (Figure 6).

The visualization result of the device doping distribution (Figure 5) clearly shows the structural design basis of the P-N junction. The device is based on a $60\mu m$ -diameter circular GaAs chip and simplified to a 2D rectangular model with a thickness of $10\mu m$ and a width of $30\mu m$ due to cylindrical symmetry. In the figure, the p-type doped region is marked in blue, and the n-type doped region is marked in red. The bottom $7.5\mu m$ region of the device is n-type doped, and the top $2.5\mu m$ region is p-type doped, with both regions having a doping concentration of 1×10^{18} cm⁻³.

To avoid carrier transport barriers caused by abrupt doping, the model uses a decay length design of $2\mu m$ to form a smoothly transitioned active light-emitting area (width: approximately 4- $5\mu m$). This heavily doped layered structure not only enhances carrier mobility but also provides sufficient recombination space for subsequent electroluminescence. Meanwhile, the symmetric doping distribution is consistent with the 2D axisymmetric modeling logic, which can reduce the interference of edge effects on current distribution and ensure the accuracy of electrical characteristic testing.

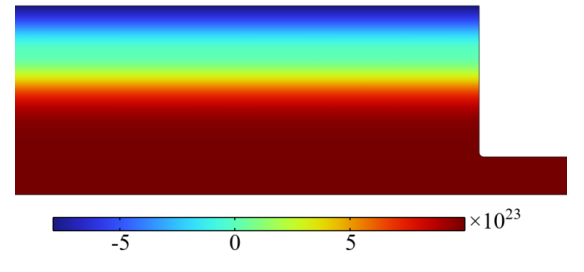


Figure 5 Geometric shape of the device

Based on the above doping structure, the I-V curve obtained by scanning the forward bias voltage from 0 V to 1.5 V (Figure 6) exhibits typical diode unidirectional conduction characteristics, which can be divided into three key stages:

When the bias voltage is lower than 1.2 V, the device current is always close to zero, in the cutoff state. The core physical mechanism of this stage is that the built-in electric field of the P-N junction is not fully offset by the external bias voltage. The heavy doping of GaAs materials (both ptype and n-type concentrations are 1×10^{18} cm⁻³) leads to a high built-in potential of the P-N junction, and the external bias voltage must first overcome this potential to drive carriers across the junction barrier. At this time, the injected electrons and holes cannot form an effective recombination current, so the device has almost no current output, only a weak leakage current. This is consistent with the reverse cut-off or forward low-voltage cut-off characteristics of an ideal diode.

When the bias voltage rises to approximately 1.2 V, the curve shows an obvious inflection point, and the current begins to increase sharply, indicating that the device enters the on-state. The 1.2 V is the turn-on voltage of this GaAs P-N junction infrared LED. This value is compatible with the bandgap of GaAs (approximately 1.43 eV) and heavy doping conditions-heavy doping increases the built-in potential of the P-N junction, requiring a higher external bias voltage to initiate effective carrier transport, which is consistent with the typical electrical characteristics of infrared LEDs.

After entering the on-state, the current increases exponentially with the bias voltage: when the bias voltage is 1.3 V, the current is approximately 5 mA; when the bias voltage rises to 1.5 V, the current further increases to 15 mA. This variation law is highly consistent with the forward characteristic of the ideal diode equation, where q is the electron charge, k is the Boltzmann constant, and T is the absolute temperature. It reflects the physical process of rapid recombination of carriers to form a current after they cross the barrier. The smoothly transitioned doping region in Figure 5 reduces carrier transport resistance, ensuring the continuity and regularity of current growth.

From the perspective of application adaptation, the characteristics of the I-V curve provide a clear basis for voltage selection in different scenarios. The bias voltage range of 1.2-1.3 V corresponds to a low current of less than 5 mA, which can not only meet the basic requirement of infrared signal transmission for household remote controls (remote controls do not require extremely high brightness, only stable signal transmission) but also minimize device power consumption and extend battery life. Therefore, it can be used as the optimal operating voltage range for low-power household scenarios.

For high-brightness scenarios such as infrared night-vision monitoring, the device needs to be driven at a higher current (e.g., 15 mA, corresponding to a bias voltage of 1.5 V). Although this can improve the total emissivity, it is necessary to accept the cost of a significant decline in IQE. Meanwhile, the problem of "emission light concentrating beneath the opaque p-type contact under high voltage" mentioned in Section 3.2 needs to be solved simultaneously-by replacing the p-type contact material with an infrared-transparent material or adjusting the contact geometry to an annular shape, light occlusion can be reduced, and "high brightness + relatively high efficiency" light output can be achieved under high current.

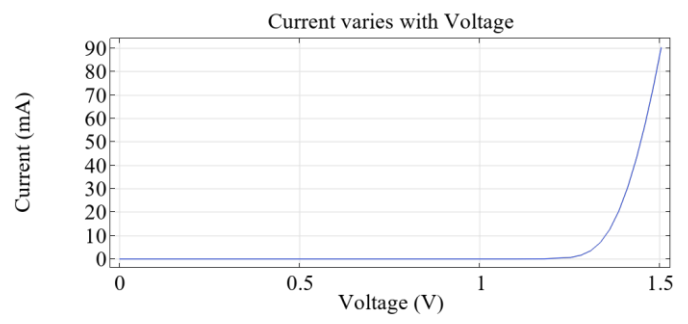


Figure 6 Geometric shape of the device

3.2 Spatial Distribution Characteristics of Emissivity

The spatial distribution of emissivity directly determines the light extraction efficiency and actual light-emitting effect of the GaAs P-N junction infrared LED. This section analyzes the law of emission distribution and its underlying physical mechanism, and clarifies the core light-emitting region of the device and application adaptation logic by combining 2D emissivity diagrams (Figs. 7, 8) under different bias voltages and 3D visualization results (Figure 9).

Under low bias voltage conditions (1.2 V, corresponding to current <5 mA), the device emissivity exhibits a uniform distribution characteristic. It can be clearly observed from Figure 8 that the radiative recombination region covers the entire p-type layer, and the region with the highest luminous intensity is concentrated in the transition zone between the p-type and n-type regions.

The core reason for this phenomenon is that under low current, the injected electrons and holes are uniformly transported in the p-type layer. Combined with the doping design in Figure 5, the p-type and n-type regions form an active area with a width of approximately 4-5µm through a 2µm decay length. Carriers do not accumulate significantly in this region and can fully recombine with holes, thereby distributing the emitted light over most of the p-type layer. At the same time, this uniform distribution avoids the central opaque p-type contact (metal disk), and most of the emitted light can escape directly from the top surface of the device without penetrating the metal contact. Therefore, the light extraction efficiency is high, which fully meets the demand for "low power consumption + stable light output" of household remote controls.

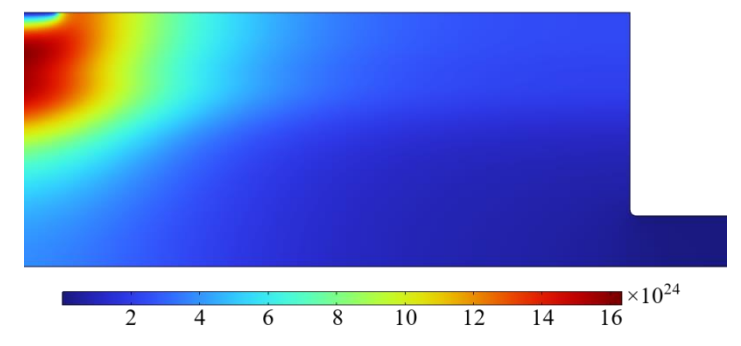


Figure 7 Emissivity of the entire device under a bias voltage of 1.5 V

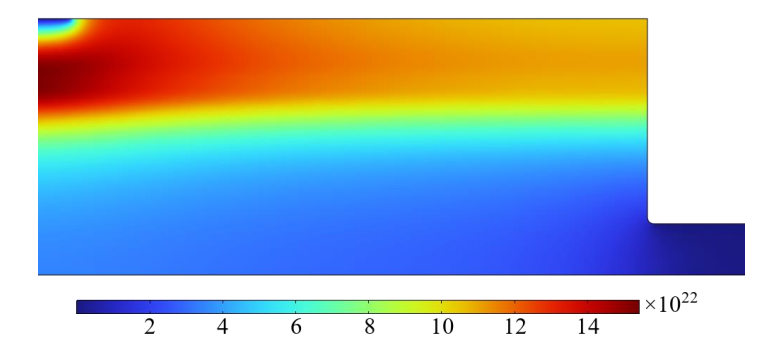


Figure 8 Emissivity of the entire device under a bias voltage of 1.2 V

When the bias voltage rises to 1.5 V (high voltage, corresponding to a current of 15 mA), the emissivity distribution changes significantly. From the 2D surface diagram in Figure 7, radiative recombination is no longer distributed uniformly over the entire p-type layer but concentrates in a small area beneath the central p-type contact. The 3D visualization results obtained by 2D rotation (Figure 9) further show intuitively that this concentrated region is distributed in a cylindrical shape along the device's axis of symmetry, with high luminous intensity but a narrow spatial range.

The physical mechanism of this change is directly related to the law of carrier transport: under high bias voltage, the external electric field intensity increases significantly, and the injected carriers are driven by the strong electric field to migrate rapidly toward the vicinity of the central p-type contact with lower potential, resulting in the dense accumulation of carriers beneath the contact and thus the contraction of the radiative recombination region. However, since the p-type contact uses an opaque metal material (e.g., aluminum), the emitted light beneath it is completely blocked by the metal and cannot escape from the top surface of the device. Even though the total emissivity increases due to the rise in current, the actual extractable light intensity decreases significantly, forming a contradiction of "high emissivity but low light output".

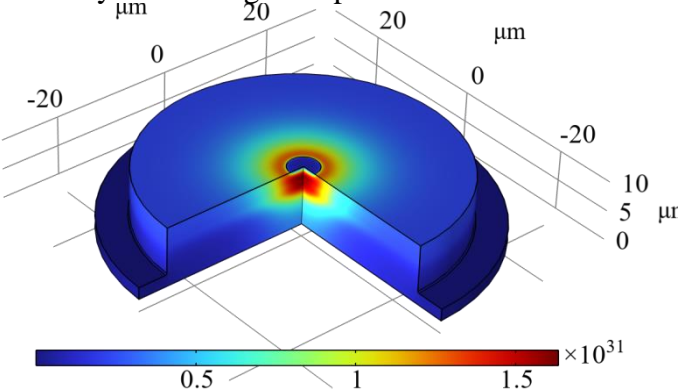


Figure 9 Emissivity of the entire device under an applied voltage of 1.5 V (3D view)

It is worth noting that regardless of the bias voltage level, the region with the highest emission intensity always corresponds to the p-n transition zone (active area) in Figure 5. This law verifies the physical nature that the P-N junction is the core of infrared LED light emission-after electrons are injected from the n-type region and holes from the p-type region, effective recombination and radiation can only occur near the junction region. The smoothly transitioned doping design in Figure 5 provides sufficient space for carrier recombination, ensuring the basic intensity of the emitted light.

From the perspective of application adaptation, the uniform emission distribution under low bias voltage is more suitable for scenarios such as remote controls that prioritize light extraction efficiency; if the device is to be used in high-brightness scenarios such as infrared night-vision monitoring, optimization is required for the problem of "emission concentration + contact occlusion" under high bias voltage. For example, replacing the p-type contact material with infrared-transparent material or adjusting the contact geometry to an annular shape can avoid occluding the central light-emitting region, providing a clear direction for subsequent device design optimization.

3.3 Mapping Effect Verification and Color Gamut Analysis

Total emissivity and internal quantum efficiency (IQE) are core indicators for evaluating the luminous efficiency of GaAs P-N junction infrared LEDs: the former reflects the total intensity of radiative recombination of the device, and the latter reflects the proportion of injected carriers that emit light through radiative recombination. The variation laws of the two directly determine the adaptability of the device in different scenarios.

This section analyzes the intrinsic logic of efficiency changes by combining the total emissivity vs. current diagram (Figure 10), IQE vs. current diagram (Figure 11), and the Auger recombination mechanism set in the model. Meanwhile, the application direction is clarified by combining the electrical and emission distribution characteristics discussed earlier.

Total emissivity is calculated by integrating the spontaneous emissivity over the entire device domain. Its correlation with current is shown in Figure 10: in the low-current stage (current <5 mA,

corresponding to a bias voltage of 1.2-1.3 V), the total emissivity increases approximately linearly with current. This is because the number of injected carriers is small at this stage, and most carriers can generate light through radiative recombination in the P-N junction active area, so the increase in emissivity is synchronized with the increase in the number of injected carriers.

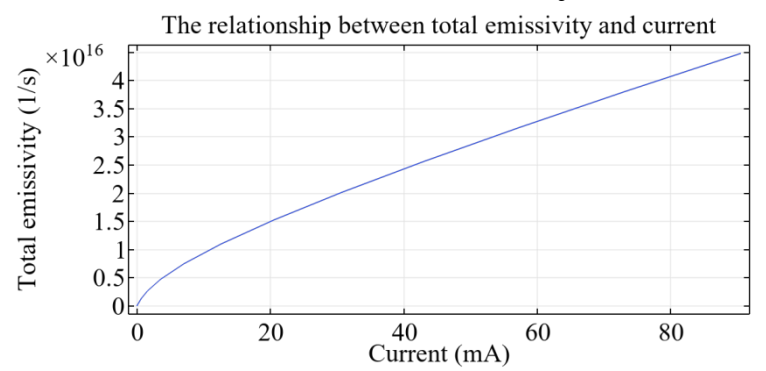


Figure 10 Relationship between total emissivity and current

When the current exceeds 5 mA, the growth slope of total emissivity slows down significantly, showing a "sublinear" growth characteristic. This phenomenon is called "efficiency droop" of LEDs, which means that the increase in carriers is no longer fully converted into the enhancement of emitted light. Some carriers are lost due to non-radiative recombination processes and cannot participate in light generation.

The variation of IQE further reveals the core mechanism of efficiency degradation, as shown in Figure 11: when the current is lower than 5 mA, the IQE remains at a high level (close to 0.35), indicating that approximately 35 out of every 100 injected carriers emit light through radiative recombination, and the impact of non-radiative recombination is negligible. When the current exceeds 5 mA, the IQE drops sharply with the increase in current and finally stabilizes at approximately 0.075, meaning that only 7.5% of carriers can emit light effectively under high current.

This change is directly related to the Auger recombination mechanism introduced in the model. Auger recombination is a non-radiative recombination process whose rate is proportional to the cube of the carrier density, while the radiative recombination rate is only proportional to the square of the carrier density. As the current increases, the carrier density in the device increases significantly, and the growth rate of the Auger recombination rate far exceeds that of the radiative recombination rate, causing non-radiative recombination to dominate the total recombination process and the IQE to drop sharply. This is also the fundamental reason for the sublinear growth of total emissivity in Figure 10.

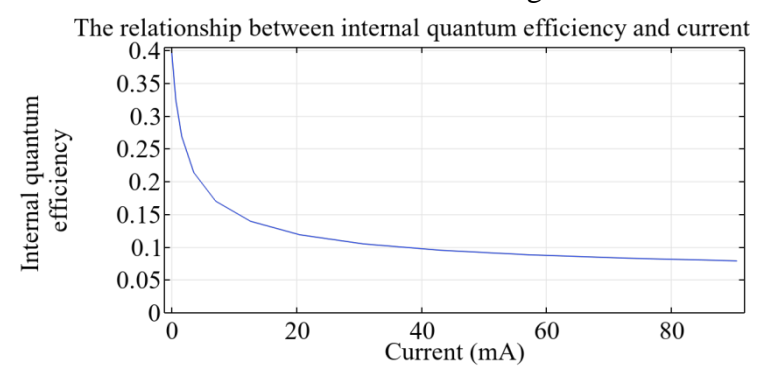


Figure 11 Schematic diagram of the relationship between internal quantum efficiency and current

From the perspective of application adaptation, the variation laws of total emissivity and IQE provide a clear basis for the selection of device operating parameters: the low-current range (<5 mA,

corresponding to a bias voltage of 1.2-1.3 V) is the optimal choice for balancing efficiency and power consumption. At this time, the IQE is high, and the total emissivity can meet the infrared signal transmission requirements of household remote controls. Meanwhile, low current can significantly extend the battery life of the device, which is highly consistent with the "low power consumption first" usage scenario of remote controls.

If the device is to be used in high-brightness scenarios such as infrared night-vision monitoring, it needs to be driven at a higher current (e.g., 15 mA, corresponding to a bias voltage of 1.5 V). Although this can improve the total emissivity, it is necessary to accept the cost of a significant decline in IQE. Additionally, the problem mentioned in Section 3.2-"emitted light concentrating beneath the opaque p-type contact under high voltage"-needs to be solved simultaneously. By replacing the p-type contact material with an infrared-transparent material or adjusting the contact geometry to an annular shape, light occlusion can be reduced, avoiding the waste of emitted light under high current and achieving "high brightness + relatively high efficiency" light output.

In summary, the sublinear growth of total emissivity and the sharp drop of IQE are both caused by non-radiative losses dominated by Auger recombination. This law not only verifies the rationality of the physical mechanism settings in the model but also provides quantitative support for the scenario-based design of GaAs P-N junction infrared LEDs-low-power scenarios need to focus on high IQE under low current, while high-brightness scenarios need to balance current, IQE, and light extraction efficiency.

4. Conclusions

Based on the 2D axisymmetric simulation of GaAs P-N junction infrared LEDs, this study systematically investigates the electrical characteristics, spatial distribution of light emission, and luminous efficiency mechanisms of the device to meet the performance optimization requirements of household infrared devices. A modeling scheme that balances computational efficiency and simulation accuracy is constructed, and the device parameter adaptation logic for different application scenarios is clarified, providing theoretical and technical support for the design of low-power and high-brightness infrared LEDs.

- (1) In the 2D axisymmetric modeling and electrical characteristic analysis, through cylindrical symmetry simplification (converting a 60μm-diameter circular chip into a 10μm-thick and 30μm-wide rectangular model) and combining with a semiconductor initialization study to achieve adaptive mesh refinement in the P-N junction area (Figure 3), the simulation accuracy and computational cost are effectively balanced. The current-voltage (I-V) curve obtained from the simulation (Figure 5) shows that the device has a turn-on voltage of approximately 1.2 V. A low bias voltage (1.2-1.3 V) corresponds to a low current of <5 mA, which meets the core low-power requirement of household remote controls; the current rises to 15 mA under a high bias voltage (1.5 V), which can be adapted to high-brightness scenarios.
- (2) For the spatial distribution law of emissivity, analysis of 2D and 3D visualization results under different bias voltages shows that: under low bias voltage (1.2 V), the emitted light is uniformly distributed over the entire p-type layer and avoids the central opaque p-type contact, resulting in high light extraction efficiency; under high bias voltage (1.5 V), the emission concentrates in a cylindrical region beneath the central p-type contact. Although the total emission intensity increases, the metal contact occlusion leads to the loss of actual light output. Meanwhile, the optimization direction for high-brightness scenarios is clarified: transparent p-type contact materials or annular contact structures can be used to reduce light occlusion and improve effective light output.
- (3) In the study of total emissivity and IQE mechanisms, integral calculation and efficiency quantitative analysis show that the total emissivity exhibits a "linear growth under low current -

sublinear growth under high current" characteristic. The IQE remains at approximately 0.35 under low current (<5 mA) and drops sharply to 0.075 under high current (>5 mA). The core reason is that the Auger recombination (non-radiative recombination) rate grows with the cube of the carrier density, far exceeding the radiative recombination rate. This conclusion clarifies the key mechanism of device efficiency degradation and provides quantitative basis for scenario-based parameter selection: the bias voltage of 1.2-1.3 V (low current and high IQE) is preferred for low-power remote control scenarios; for high-brightness scenarios such as night-vision monitoring, high current driving is required, and contact structure optimization should be combined simultaneously to balance brightness and efficiency.

The application value of this research is reflected in three aspects: 2D axisymmetric modeling can be directly used for the rapid simulation verification of low-cost household infrared LEDs; the law of emissivity distribution provides a clear path for contact structure optimization; the efficiency mechanism analysis provides a quantitative standard for bias voltage and current selection in different scenarios. In the future, multiple non-radiative recombination mechanisms such as lattice scattering and impurity scattering can be further introduced, or the simulation can be extended to GaAs-based heterojunction infrared LEDs to adapt to the design requirements of more complex high-performance infrared optoelectronic devices.

Acknowledgments

This study was supported by Innovation and Entrepreneurship Training Program for Undergraduates' at Yingkou Institute of Technology under Grant (S202414435029, Project Title: The Design of LED Flash Power Supply).

References

- [1] Si X L, Huang W X, Zhang L M, et al. Research on on-board relative radiometric calibration method based on LED point light source[J/OL]. Acta Photonica Sinica, 1–13 [2025-07-07].
- [2] Zhang Z Y. Research on the influence of optical design on LED lighting efficacy improvement[J]. China Light & Lighting, 2025, (06): 90–92 + 171.
- [3] Huangfu X H, Liu S F, Xiao J J, et al. Regulation of infrared photoelectric properties of GaInAsSb p-n junctions by nanophotonic structures[J]. Acta Physica Sinica, 2021, 70(11): 348–356.
- [4] Cheng X D, Chen Z K, Zhang Z L, et al. Research progress of MicroLED based on quantum dot color conversion layer[J]. Advances in New and Renewable Energy, 2025, 13(01): 107–120.
- [5] Wang Y L. Design, synthesis of p-n junction conjugated polymer materials and their application in supercapacitors[D]. Peking University, 2019.
- [6] Yang L. Investigation on the construction of p-n heterojunctions and direct Z-scheme heterojunctions and carrier migration[D]. Shaanxi Normal University, 2022.
- [7] Jiang X G, Li B Q, Deng Z J, et al. Study on spectral and spatial uniformity of near-infrared annular LEDs[J]. Light & Lighting, 2025, (05): 95–98.
- [8] Sun J F, Ji S J, Meng Z H, et al. Regulation of broadband near-infrared region I emission and near-infrared LED device application of $(Sr, Ba)_3MgTa_2O_9$: Cr^{3+} by Sr^{2+}/Ba^{2+} substitution[J]. Chinese Journal of Luminescence, 2024, 45(12): 1956–1965.
- [9] Li Z, Gao Y Z, Zhang J Y. Multi-spectral complex infrared scene simulation technology[J]. Acta Optica Sinica, 2023, 43(15): 206–222.
- [10] Yu H B, Peng Z L. Design and research of LED constant current driving power supply based on HPLC[J]. Automation & Instrumentation, 2025, (09): 114–116 + 122.